Title: AKAP350 regulates LFA-1 organization during NK cytolytic response

Authors: Alejandro P. Pariani[1], Evangelina Almada[1], Florencia Hidalgo[1], Carla Borini-Etichetti[1], Rodrigo Vena[2], Leandra Marín[1], Cristián Favre[1], James R. Goldenring[3], M. Cecilia Larocca[1]*

Affiliation: [1]Instituto de Fisiología Experimental, Consejo Nacional de Investigaciones Científicas y Técnicas (CONICET), Facultad de Ciencias Bioquímicas y Farmacéuticas, Universidad Nacional de Rosario (UNR), (2000) Rosario, Argentina.

[2] Instituto de Biología Molecular y Celular de Rosario, CONICET, Facultad de Ciencias Bioquímicas y Farmacéuticas, UNR, Rosario, Argentina.

[3] Epithelial Biology Center and Department of Cell & Developmental Biology, Vanderbilt University School of Medicine, Nashville, Tennessee, USA

Corresponding Author's Information: M. Cecilia Larocca, Instituto de Fisiología Experimental, Facultad de Ciencias Bioquímicas y Farmacéuticas. Suipacha 570, 2000 Rosario, Argentina. Tel: 54-341-4305799. E-mail: larocca@ifise-conicet.gov.ar

Abstract

Natural killer (NK) cell cytotoxicity requires extensive cytoskeleton remodeling and membrane receptor reorganization at the NK-target cell immune synapse (IS). The lymphocyte function–associated antigen (LFA)-1 accumulates at that structure, playing a central role in NK-IS assembly. The mechanisms underlying LFA-1 accumulation at the IS remain unclear. We found that AKAP350, a centrosome/Golgi associated protein, enabled NK-cytolytic activity by facilitating LFA-1 organization at the IS. Our results revealed the existence of an intracellular pool of LFA-1 that colocalized with the Golgi apparatus, which redistributed to the IS pole in control, but not in cells with decreased expression or localization of AKAP350 at the Golgi apparatus. Similarly to what was described in other cells, our results showed that NK cells nucleated microtubules at the Golgi apparatus in an AKAP350-dependent manner. Concomitantly, AKAP350 delocalization from the Golgi apparatus or pharmacological disruption of microtubule dynamics or Golgi integrity impaired LFA-1 localization at the IS. Altogether, our results unveil a novel mechanism of LFA-1 reorganization relevant for NK-cell activation, revealing the participation of the Golgi apparatus in NK-lytic IS maturation.

Introduction

Natural killer cells (NK) are the cytolytic effectors of the innate immune system, which constitute the first line of immunological defense and are particularly relevant for the elimination of viral infected and neoplastic cells. NK cytotoxic effector function relies on the formation of a specialized junction with its target cell, generally referred to as immune synapse (IS). The formation and maturation of NK-IS requires the participation of NK receptors, signalling molecules and cytoskeletal elements, which accumulate in distinct regions within the IS to form a supramolecular activation cluster (SMAC), distinctly organized at peripheral (pSMAC) and central (cSMAC) zones (Orange, 2008). The persistent outside-in signaling generated by the interaction of NK activating receptors with their ligands in the target cell at the IS, in a context of absence of inhibitory signals, triggers a multistep, highly regulated process that culminates with the directed secretion of lytic molecules contained in specialized lysosomes (lytic granules) through the cSMAC into the target cell (Mace et al., 2014). The initial contact between NK and target cells may involve any of a number of different receptors, among which the integrin leukocyte functional antigen (LFA)-1 is of particular interest. LFA-1 is a heterodimer consisting of αL (CD11a) and β2 (CD18) chains, which is essential for the stabilization of the NK contact with the target cell (Hoffmann et al, 2011). In addition to mediating the tight adhesion to target cells, LFA-1 contributes to NK cytotoxic response by initiating signaling pathways that promote lytic granule convergence to the centrosome and lytic granule/centrosome polarization towards the IS (Barber et al., 2004; Bryceson et al., 2005). LFA-1 reorganization implies conformational changes that lead to an activated configuration, as well as an increase in its localization at the NK-target cell contact site. The implication of different NK receptors and interleukins in the inside out signaling that leads to LFA-1 activation has been well established (Urlaub et

al, 2017). Nevertheless, the cellular mechanisms underlying the increase in LFA-1 expression at the IS in this context remain unclear.

A major mediator of NK cell cytolytic activity is the cytoskeleton. In this regard, the role of actin dynamics on the maturation of the lytic IS has been well established (Lagrue el al, 2013). Regarding the microtubule cytoskeleton, its dynamics during NK activation has not been thoroughly analyzed and it remains unclear whether they serve any role other than facilitating the delivery of lytic granules to the synaptic cleft (Chen et al., 2006; Stinchcombe et al., 2006). The A-kinase anchoring protein 350 (AKAP350), also known as AKAP450, CG-NAP or AKAP9, is a centrosome and Golgi apparatus-scaffold protein (Schmidt et al, 1999) with a prominent role in microtubule remodeling: AKAP350 participates in microtubule nucleation (Takahashi et al., 2002, Rivero et al., 2009, Kolobova et al., 2019), in the regulation of microtubule growth (Larocca et., al 2006), in mitotic spindle orientation (Almada et al., 2017), and in centrosome translocation in different cell contexts (Robles Valero et al., 2010, Tonucci et al., 2015). The first study in immune cells that revealed AKAP350 participation in the regulation of their effector functions was performed in migratory T cells (El Din El Homasany et al., 2005). Those studies demonstrated that the interference with AKAP350 function at the centrosome leads to inhibition of LFA-1 induced-cell migration. Later studies indicated that, during antigen recognition by T-cells, AKAP350 participates in LFA-1 activation and centrosome translocation towards the IS (Robles Valero et al., 2010). Regarding the mechanisms involved, they have not been elucidated.

In the present study we analyzed AKAP350 participation in the development of NK cytotoxic effector function and characterized its role in microtubule cytoskeleton

remodeling and LFA-1 reorganization at the lytic IS. Our results further reveal a novel role for the Golgi apparatus and its associated microtubules in NK lytic IS maturation.

Results

1. AKAP350 localization at the Golgi apparatus in NK/YTS cells is up-regulated during cell activation

To determine if AKAP350 could participate in NK cytotoxic response, we first evaluated its expression in YTS immortalized NK cells. Western blot analysis of YTS cell-extracts confirmed AKAP350 expression at protein level. Immunofluorescence analysis of AKAP350 staining in resting YTS cells showed that AKAP350 colocalized with γ-tubulin and GM-130, what is indicative of AKAP350 localization at the centrosome and at the Golgi apparatus (Figure 1A, B first row). KT86 cells are derived from K562 erythroleukemia cells and constitute susceptible targets for YTS cells. The analysis of YTS:KT86 conjugates indicated that AKAP350 localization at the centrosome was reduced (-50%), whereas its localization at the Golgi apparatus was increased (+44%) in activated NK cells (Figure 1A, B, second row). These results suggest that NK cell activation induces a partial translocation of AKAP350 from the centrosome to the Golgi apparatus.

2. Decrease of endogenous AKAP350 expression impairs NK cytolytic activity

To analyze the impact of AKAP350 expression in the development of NK cytolytic effector function, we generated YTS cells with decreased AKAP350 expression (AKAP350KD) using a lentiviral short hairpin RNA expression system for targeting two different AKAP350 mRNA sequences, as we have previously described (Tonucci et al., 2015). Western blot analysis of AKAP350 protein levels showed that the expression of either shRNA1 or shRNA4 efficiently decreased AKAP350 levels to less

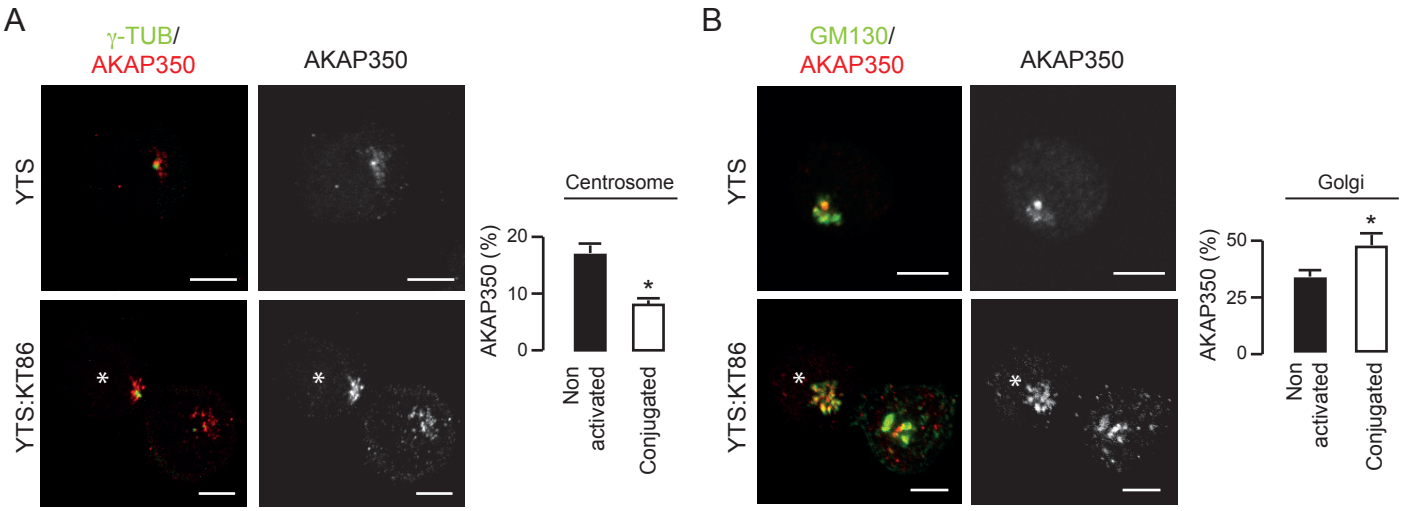

Figure 1. AKAP350 localization in YTS cells. Isolated YTS cells or YTS:KT86 conjugates were stained and analyzed by confocal microscopy as described in Materials and Methods. A,B) Merge images show YTS cells (upper row) or YTS:KT86 conjugates (lower row) staining for AKAP350 (red) and γ-tubulin (A) or GM130 (B) (green). Asterisk denotes YTS cells in YTS:KT86 conjugates. Bars represent the mean fraction of AKAP350 fluorescence present at centrosomes (A) or at the Golgi apparatus (B) in isolated or conjugated YTS cells, expressed as percentage of total AKAP350-fluorescence. Results are representative of three independent experiments. At least 20 cells were analyzed for each experiment. Error bars represent SEM. *$p < 0.05$. Scale bars, 5 μm.

than 10% of control levels (Figure 2A). To assess AKAP350 participation in the formation in NK: target cell conjugates, control or AKAP350KD YTS cells were labeled with TrackerTM Deep Red and KT86 cells were labeled with CFSE. Cells were incubated at different NK:target cell ratios, for different periods, and the formation of cell conjugates positive for both fluorophores was analyzed by FACS. Our results showed that the decrease in AKAP350 expression did not elicit any evident effect in the initial adherence between NK and their susceptible target cells (Supplementary Figure 1). In order to analyze NK cytolytic activity in those conditions, control and AKAP350KD YTS cells were incubated with CFSE-labeled KT86 cells and target cell lysis was analyzed by FACS analysis of propidium iodide stained cells (Figure 2B,C). Our results showed that the decrease in AKAP350 levels by expression of either shRNA1 or shRNA4 impaired NK cytolytic activity.

Considering that lytic granule translocation towards the IS is an essential step in NK cytolytic response, lytic granule localization was evaluated in control and AKAP350KD YTS cells which were conjugated to CFSE-labeled KT86 target cells. The IS was defined as the region of YTS/KT86 contact delimited in the DIC channel, and perforin and γ-tubulin staining were used to identify lytic granules and the centrosome, respectively. The average distance between lytic granules and the IS was increased in AKAP350KD cells, thus indicating decreased lytic granule translocation to the IS in these cells (Figure 3A). Regarding the steps that lead to lytic granule translocation to the IS, both lytic granule convergence to the centrosome and centrosome translocation towards the IS were impaired, as denoted by the increased distance from lytic granules to the centrosome (Figure 3A) and from the centrosome to the IS in AKAP350KD cells (Figure 3B). Therefore, AKAP350 enables NK cytolytic function by participating in

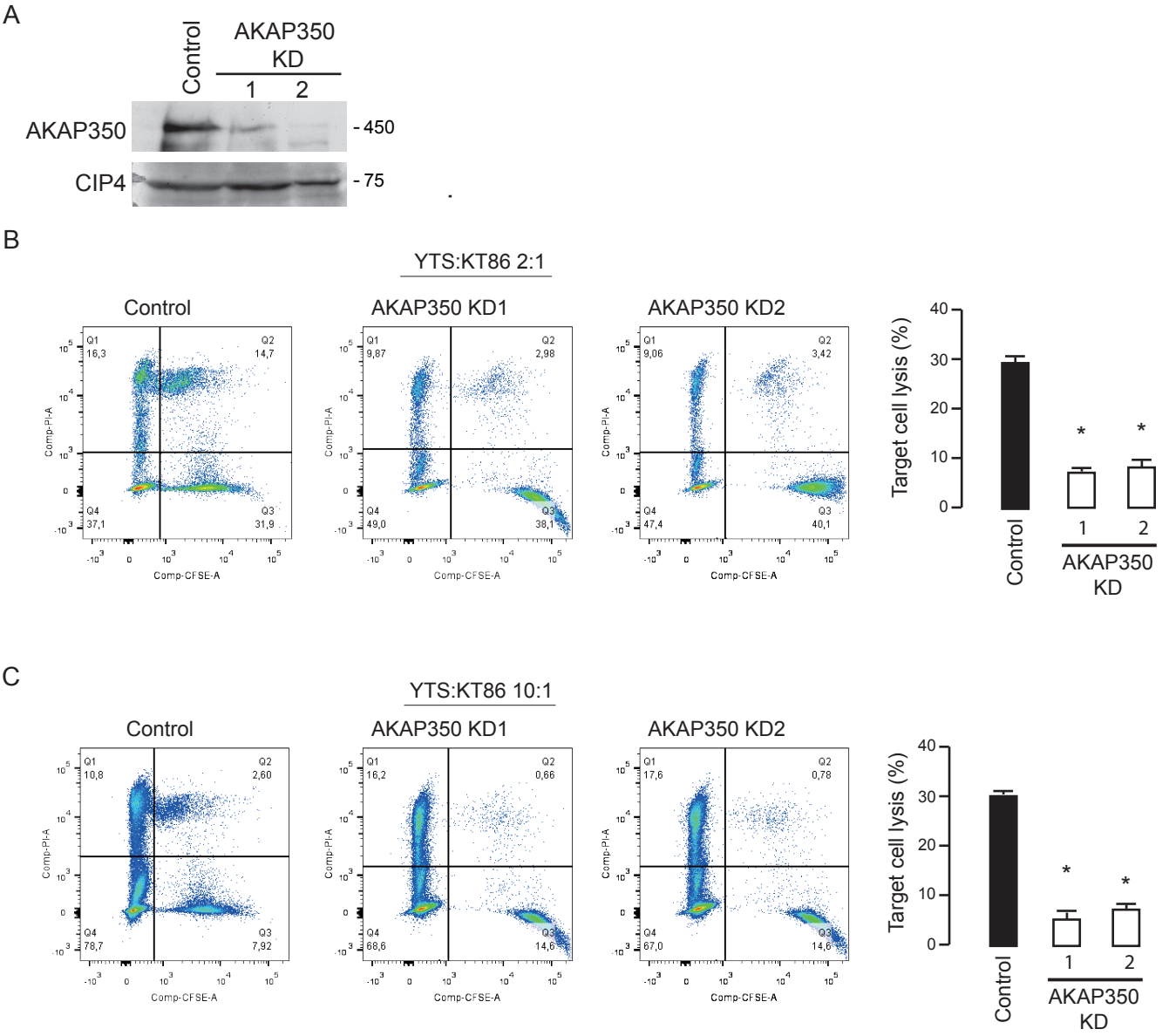

Figure 2. Reduction of AKAP350 expression levels diminishes YTS cells' cytotoxicity. Two different specific shRNAs (shRNA1 and shRNA4) were used to generate YTS cells with decreased AKAP350 expression (AKAP350KD1 and AKAP350KD2, respectively), as described in Materials and methods. A) Western blot analysis of AKAP350 expression in control, AKAP350KD1 and AKAP350KD2 YTS cells. CDC42-interacting protein 4 (CIP4) was used as loading control. B,C) KT86 cells were stained with CFSE and mixed with YTS cells at effector: target ratios of 2:1 (B) or 10:1 (C). After the incubation period, cells were stained with PI and analyzed by flow cytometry. YTS cytotoxic activity was estimated as the fraction of total CFSE positive events that were also positive for PI. Bars chart represents the mean percentage of double positive events for control, AKAP350KD1 and AKAP350KD2 cells, representative of three independent experiments. Error bars represent SEM. *$p < 0.05$.

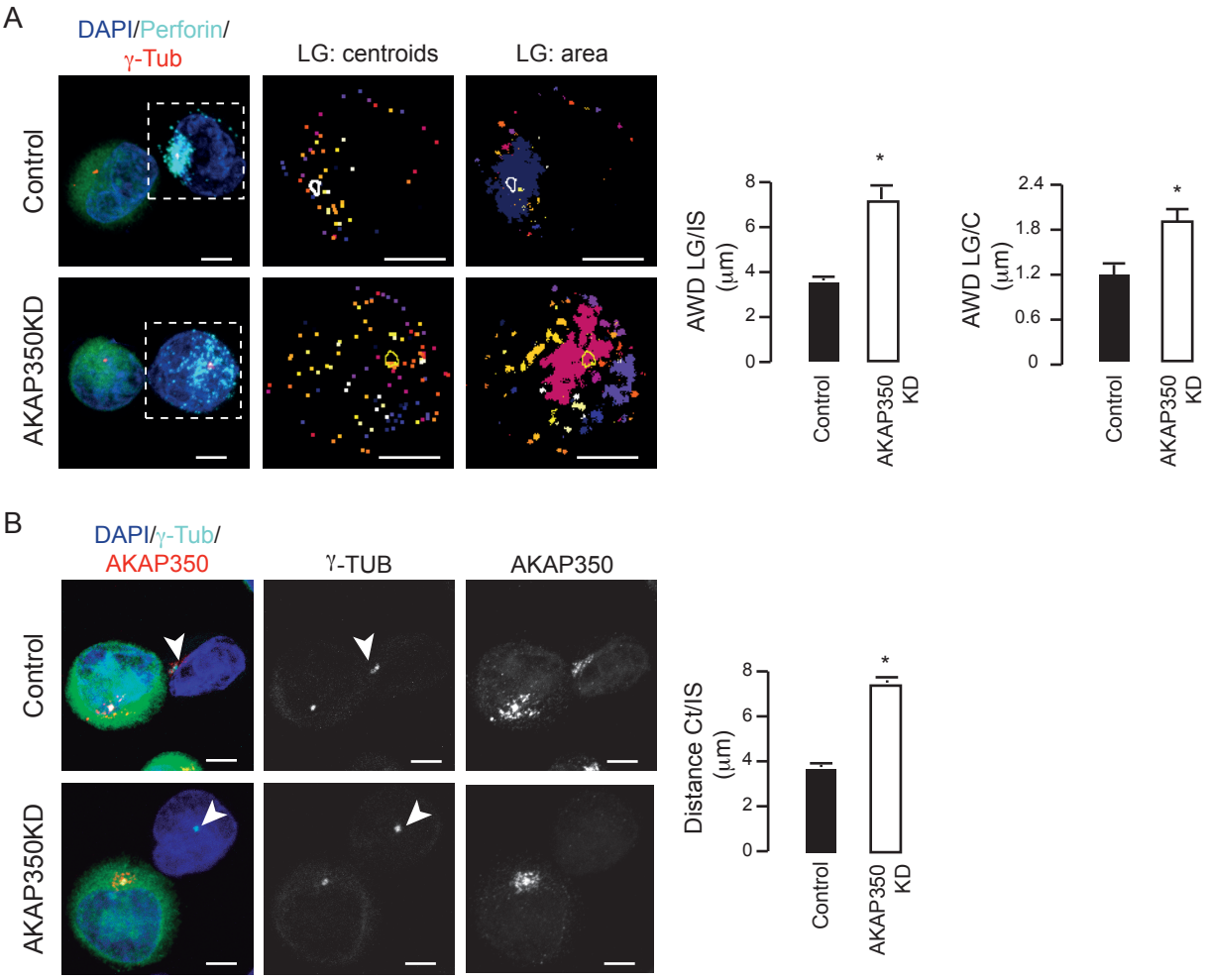

Figure 3. AKAP350 is required for lytic granule convergence and centrosome polarization during YTS cell-activation. Control and AKAP350KD YTS cells were incubated with CFSE labeled KT86 cells at a YTS:KT86 2:1 ratio. Cell conjugates were fixed, stained and analyzed by confocal microscopy. A) Merge images show staining for DAPI (blue), perforin (cyan) and γ-tubulin (red). The second and third columns show the localization of the centrosome, as delimited with an automatic selection tool, and the localization of the lytic granules centroids (second column) or the lytic granules area (third column), visualized using a specific image J tool, corresponding to the boxed cell from the first column. Bars represent the mean area weighed distance (AWD) from the lytic granules to the IS or to the centrosome, calculated as described in Materials and methods. B) Merge images show staining DAPI (blue), AKAP350 (red) and γ-tubulin (cyan). White arrows indicate the position of γ-tubulin-labeled centrosomes in YTS cells. Bars represent the mean distance from the centrosome to the IS. Results are representative of four (A) or five (B) independent experiments. At least 30 conjugates were analyzed for each experiment. Error bars represent SEM. Scale bars, 5 μm. *p<0.05.

regulatory events that lead to lytic granule convergence to the centrosome and translocation to the IS.

3. The decrease in AKAP350 expression impairs LFA-1 reorganization at the IS in activated NK cells

Analysis of YTS:KT86 conjugates morphology indicated that the surface of interaction between both cells was reduced in AKAP350KD cells, which was verified by a reduction in the IS area to 50% of control levels ($p<0.01$). Consistently, LFA-1 accumulation at the IS was impaired in AKAP350KD cells (Figure 4A). Similarly, inhibition of LFA-1 reorganization was also observed in AKAP350KD cells when they were specifically activated with the LFA-1 ligand ICAM-1 (Figure 4B), thus suggesting a direct effect of AKAP350 on LFA-1 reorganization. In addition, the analysis of the 3D organization of the IS indicated that, as expected, LFA-1 clustered at the pSMAC in control cells (Vyas et al, 2001), whereas, in AKAP350KD cells, it was homogeneously distributed (Figure 4C). It is noteworthy that, as measured by western blot and immunofluorescence, neither LFA-1 expression nor its localization at the plasma membrane was affected by the decrease in AKAP350 expression (data not shown), what is in line with our results showing that the decrease in AKAP350 expression did not elicit any evident defect on YTS conjugation to KT86 cells (Supplementary Figure 1).

In order to verify if the inhibition of lytic IS maturation in AKAP350KD cells (Figure 3) was also observed when YTS cells were exclusively activated via LFA-1, we further analyzed lytic granule convergence and centrosome translocation towards the activated surface in cells specifically activated with ICAM-1. Our results showed that both processes were inhibited in AKAP350KD cells (Figure 4D). These results indicate that AKAP350 participates in LFA-1 recruitment to the lytic IS in NK cells, and, considering the role of LFA-1 in activating lytic granule translocation towards the IS

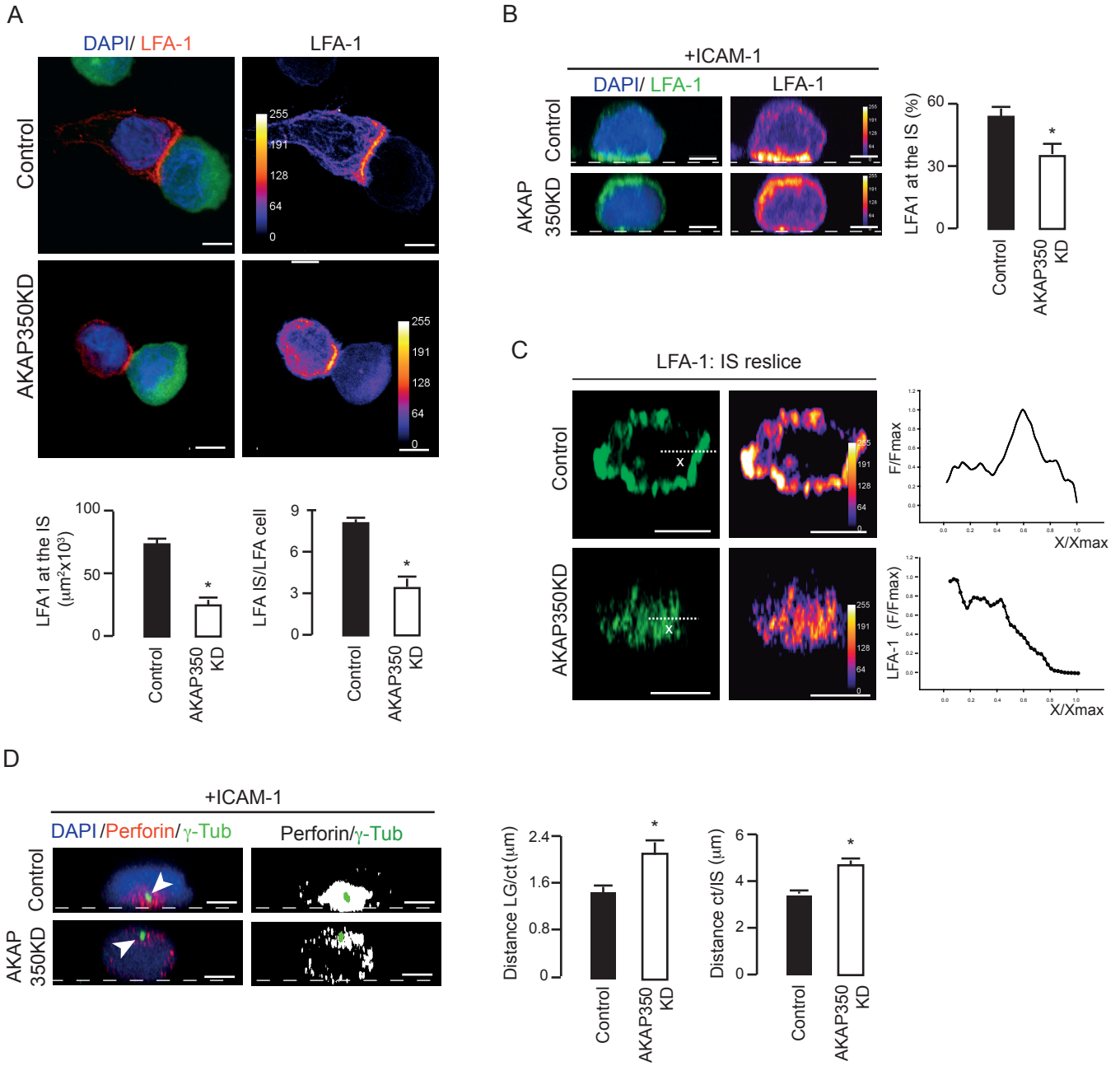

Figure 4. Reduction of AKAP350 expression levels results in defective LFA-1 organization at the IS. A) Control and AKAP350KD YTS cells were incubated with CFSE labeled KT86 cells at a 2:1 ratio. Merge images show YTS:KT86 conjugates staining for LFA-1 (red) and DAPI (blue). LFA-1 channel is shown in pseudocolor. Bars represent the mean area positive for LFA-1 at the IS and the average intensity of LFA-1 fluorescence at the IS relative to the average intensity of LFA-1 fluoresecence at the cell for four independent experiments. At least 30 conjugates were analyzed for each experiment. Error bars represent SEM. B) Control and AKAP350KD YTS cells were activated using coverslips coated with ICAM-1. Merge images show LFA-1 (green) and DAPI (blue) staining. LFA-1 channel is also shown in pseudocolor. White dashed lines indicate the cell surface in contact with the coverslip. Bars represent the mean fraction of LFA-1 fluorescence located at the cell surface in contact with the ICAM-1 coated coverslip, expressed as percentage of total cell fluorescence representative of three independent experiments. At least 30 conjugates were analyzed for each experiment. Error bars represent SEM. C) Images show the X-Z projection of the IS region corresponding to control and AKAP50KD YTS cells. LFA-1 staining is shown in green and in pseudocolor. Dashed lines denote the radius of the IS where LFA-1 and actin intensity of fluorescence were quantified. Charts represent the profile of intensity of fluorescence quantified for each channel, representative of at least ten IS analyzed in three independent experiments. D) Control and AKAP350KD YTS cells were activated using coverslips coated with ICAM-1. Merge images show γ-tubulin (green), perforin (red) and DAPI (blue) staining. The second column shows the binarized image of the perforin channel, with the ROI corresponding to the centrosome indicated in green. Bars represent the mean distance between the lytic granules and the centrosome (first chart) or between the centrosome and the ICAM-1 coated surface, representative of three independent experiments. Scale bars, 5 μm (A,B,D) or 2.5 μm (C). *p<0.05.

(Barber et al., 2004, Bryceson et al., 2005), provide evidence for that mechanism being responsible for the defective IS maturation and decreased lytic activity observed in AKAP350KD cells.

4. NK cells express an intracellular pool of LFA-1 that polarizes to the IS in an AKAP350 dependent manner

The mechanisms underlying LFA-1 accumulation at the IS in NK cells have not been clarified so far. Previous studies in naive CD8+ T cells revealed an intracellular pool of LFA-1 that can translocate to the IS upon T cell activation (Capece et al, 2017). To our knowledge, there was no data regarding the presence of a similar pool of LFA-1 in NK cells. Our analysis of permeabilized YTS cells indicated the presence of cytosolic vesicles containing LFA-1, which polarized towards the IS in control, but not in AKAP350 KD activated cells (Figure 5A). Similarly to what was described in T cells, LFA-1 vesicles partially colocalized with Rab11, indicating partial association with the recycling endosomes (Figure 5B). More interestingly, we found a prominent LFA-1 colocalization with GM130 (Figure 5C), which suggested the participation of the Golgi apparatus in LFA-1 intracellular trafficking. LFA-1 colocalization with GM130 or with Rab11 was not affected by the decrease in AKAP350KD expression, indicating that the presence and the identity of the intracellular pool was preserved in these cells (Supplementary figure 2). In order to assess the implication of the Golgi apparatus in LFA-1 recruitment to the IS in activated cells, we analyzed LFA-1 localization at the IS in NK cells that were pre-treated with Brefeldin A (BFA), a pharmacologic inhibitor of ADP-ribosylation factors that leads to the collapse of the Golgi and its redistribution into the ER (Chardin and McCormick, 1999). Analysis of LFA-1 distribution at the IS showed that BFA-treatment inhibited LFA-1 accumulation and clustering at the pSMAC (Figure 5D,E).

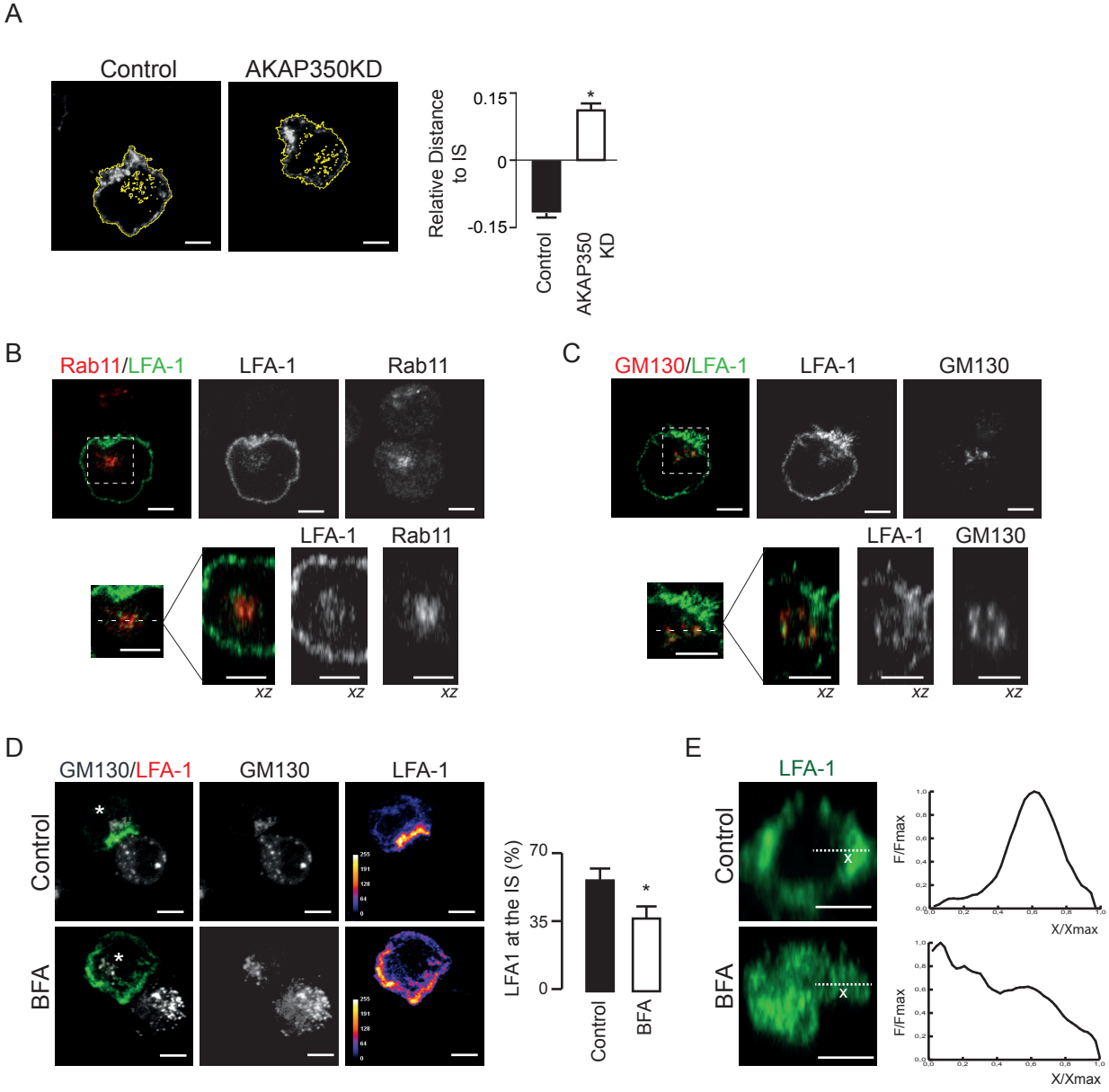

Figure 5. LFA-1 is expressed intracellularly and its redistribution to the IS is dependent on the integrity of the Golgi apparatus. A-C) Control (A-C) and AKAP350KD (A) YTS cells were incubated with KT86 cells at a 2:1 ratio. Cell conjugates were fixed, stained and analyzed by confocal microscopy. A) Images show LFA-1 staining (grey scale) and the ROIs delimiting YTS cells and the individual LFA-1 vesicles in yellow. Bars represent the mean difference between the average weighted distance (AWD) from the intracellular LFA-1 vesicles to the IS and the distance from the cell centroid to the IS, relativized to the latter, representative of three independent experiments. At least 10 conjugates were analyzed for each experiment. Error bars represent SEM. B,C) Merge images show staining for LFA-1 (green) and Rab11 (red, B) or GM130 (red, C) and the x,z orthogonal view of the boxed areas at the ordinate indicated with dashed lines. D-E) YTS cells were treated with brefeldin A (BFA) as described in Material and methods. Control or BFA treated YTS cells were incubated with KT86 cells. D) Merge images show staining for LFA-1 (green) and GM130 (gray). LFA-1 channel is also shown in pseudocolor. Bars represent the mean fraction of LFA-1 fluorescence located at the IS, expressed as percentage of total cell fluorescence for the LFA-1 channel, representative of three independent experiments. At least 8 conjugates were analyzed for each experiment. Error bars represent SEM. E) Images show the x,z projection of the IS region corresponding to control and BFA treated YTS cells. Dashed lines denote the radius of the IS where LFA-1 intensity of fluorescence was quantified. Charts represent the intensity profile of fluorescence, representative of at least ten IS. Asterisks indicate YTS cells (D-E). Scale bars, 5 μm. *p<0.05.

5. AKAP350 participates in microtubule nucleation at the Golgi apparatus in activated NK cells

Previous studies demonstrate that AKAP350 modulates microtubule nucleation at the Golgi apparatus (Rivero et al, 2009; Ori-McKenney et al, 2012; Maia et al, 2013; Tonucci et al, 2018). Although they have not been characterized in lymphocytes, in different systems Golgi derived microtubules participate in polarized vesicle trafficking towards specific plasma membrane domains (reviewed in Sanders and Kaverina, 2015). Analysis of microtubule distribution in control and AKAP350KD YTS cells indicated differences regarding microtubule-association with the Golgi apparatus (Figure 6A). In order to elucidate if those differences could be related to differences in microtubule nucleation, we first analyzed if there was microtubule nucleation at the Golgi apparatus in YTS cells, using ice recovery assays as previously described (Grimaldi et al, 2013). Cells were seeded on coverslips coated with either IgG or with ICAM-1 and an activating anti-CD28 antibody for simulating NK resting or activating conditions, respectively. Microtubule depolymerization was induced by ice incubation. Our results showed that, after 3 min of rewarming, microtubules associated with the centrosome and with the Golgi apparatus both in resting and in activated YTS cells (Figure 6B) . We further analyzed the role of AKAP350 in microtubule nucleation during YTS cell activation. After 7 min of rewarming, AKAP350KD cells showed a significant reduction in newly nucleated microtubules at the Golgi apparatus (Figure 6C, upper bars), whereas no differences were observed for centrosome-associated microtubules (Figure 6C, lower bars). Similar results were obtained at 3 min of recovery (not shown). Considering that Golgi derived microtubules show high levels of α-tubulin acetylation, we analyzed the relative levels of acetylated α-tubulin in control and AKAP350KD YTS cell lysates by western blot. In accordance with the decrease in Golgi derived

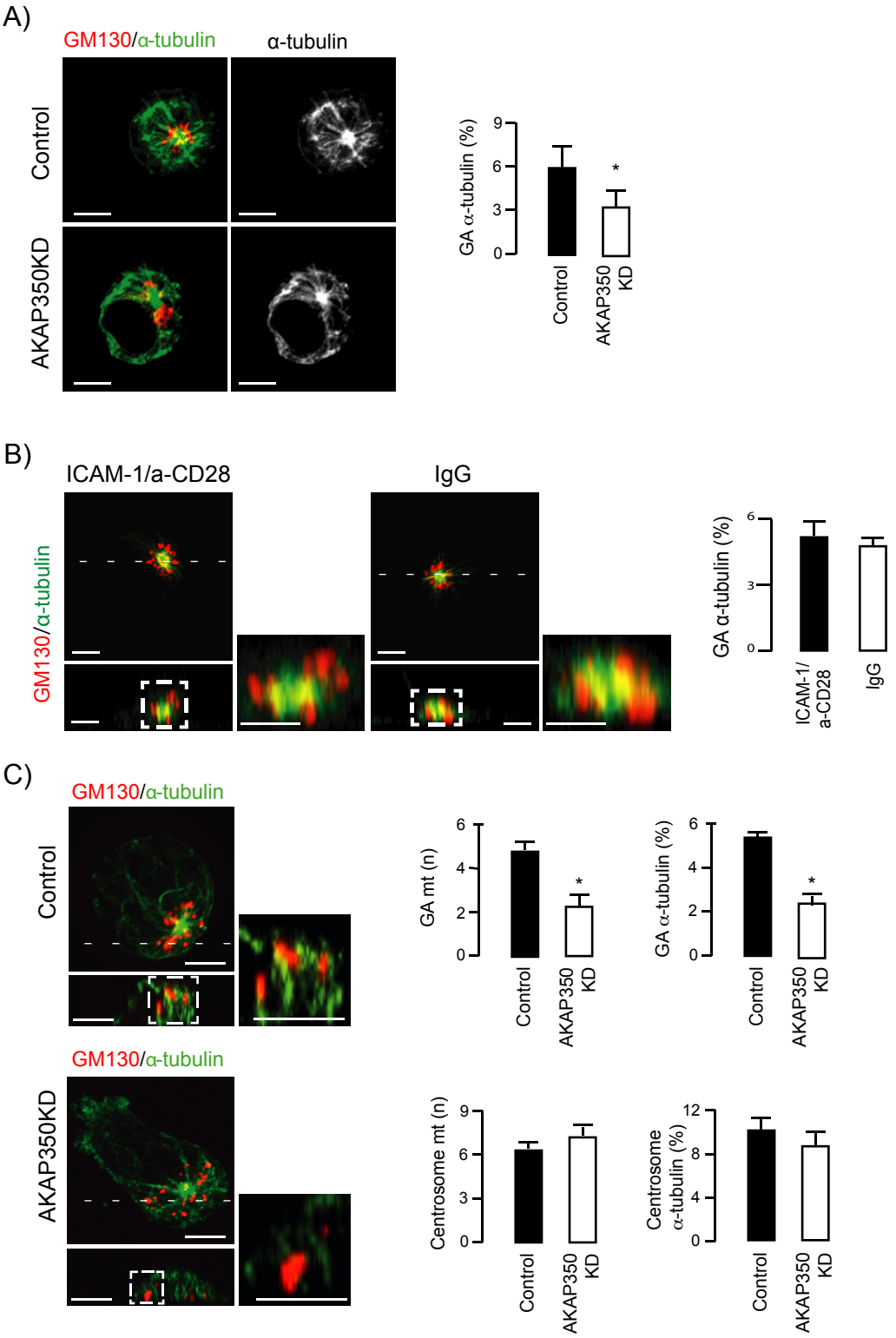

Figure 6. AKAP350 is essential for microtubules nucleation at the Golgi apparatus in activated YTS cells. A) Control and AKAP350KD YTS cells were activated for 30 minutes using coverslips coated with ICAM-1 and anti-CD28 antibody. Merge images show staining for GM130 (red) and α-tubulin (green). Bar charts represent the mean fraction of α-tubulin fluorescence that colocalized with GM130, expressed as percentage of total cell fluorescence. B) Control YTS cells were seeded on coverslips coated ICAM-1 and the activating anti-CD28 antibody (activating conditions) or with IgG (resting conditions) for 30 minutes and then subjected to ice recovery assay. C) Control or AKAP350KD YTS cells were activated on coverslips coated with ICAM-1 and the activating anti-CD28 antibody for 30 minutes and then subjected to ice recovery assays. B, C) Merge images show staining for GM130 (red) and α-tubulin (green), and the orthogonal views of the x,z reslice at the ordinate level indicated with dashed lines, for cells fixed at 3 min (B) or 7 min (C) of recovery. The insets show a higher amplification of the boxed areas, for better visualization of microtubule association to the Golgi apparatus. Bar charts represent the mean fraction of α-tubulin fluorescence associated to each organelle, expressed as percentage of total cell fluorescence for the α-tubulin channel (B,C) and the mean number of microtubules derived from the centrosome or from the Golgi apparatus (C), representative of three independent experiments. At least 10 cells were analyzed for each experiment. Error bars represent SEM. Scale bars, 5 μm. *p<0.05.

microtubules, the decrease in AKAP350 expression was associated with a decrease in the levels of acetylated α-tubulin in YTS cells (Supplementary Figure 3A).

6. AKAP350 association to the GA is essential for IS maturation in NK cells

To specifically examine the relevance of Golgi associated AKAP350 in the maturation of NK lytic IS, we prepared YTS cells with stable expression of AKAP350(1-1229) (AKAP350GBD) domain, which acts as a dominant negative construct that displaces the protein from the Golgi apparatus, inhibiting microtubule nucleation at this organelle (Hurtado et al 2011). The analysis of AKAP350 colocalization with GM130 confirmed that AKAP350 localization at the Golgi apparatus was significantly decreased in AKAP350GBD cells (Supplementary Figure 4). In accordance with the correlation between impaired Golgi nucleation of microtubules and decreased levels of acetylated described for AKAP350KD cells (Figure 6 and Supplementary Figure 3A), relative levels of acetylated α-tubulin were decreased in AKAP350GBD cells (Supplementary figure 3B). The analysis of the intracellular pool of LFA-1 showed that, whereas LFA-1 colocalization with GM130 was preserved in AKAP350GBD cells (Figure 7A), its distribution towards the IS was severely impaired in those cells (Figure 7B). Concomitantly, LFA-1 accumulation and organization at the IS was compromised in AKAP350GBD cells (Figure 7C,D). Overall, this set of data confirmed the direct involvement of the Golgi apparatus and, specifically, its associated AKAP350 in LFA-1 organization at the IS during NK cell-activation and gave strong evidence supporting a role for Golgi derived microtubules in this mechanism.

7. Microtubule cytoskeleton integrity is necessary for LFA-1 organization at the IS

Even though the effects of microtubule targeting agents on NK cells cytotoxicity have been described (Katz et al., 1982; Fong et al., 2019), and the role of microtubules as tracks that direct lytic granule translocation towards the IS has been characterized (Chen

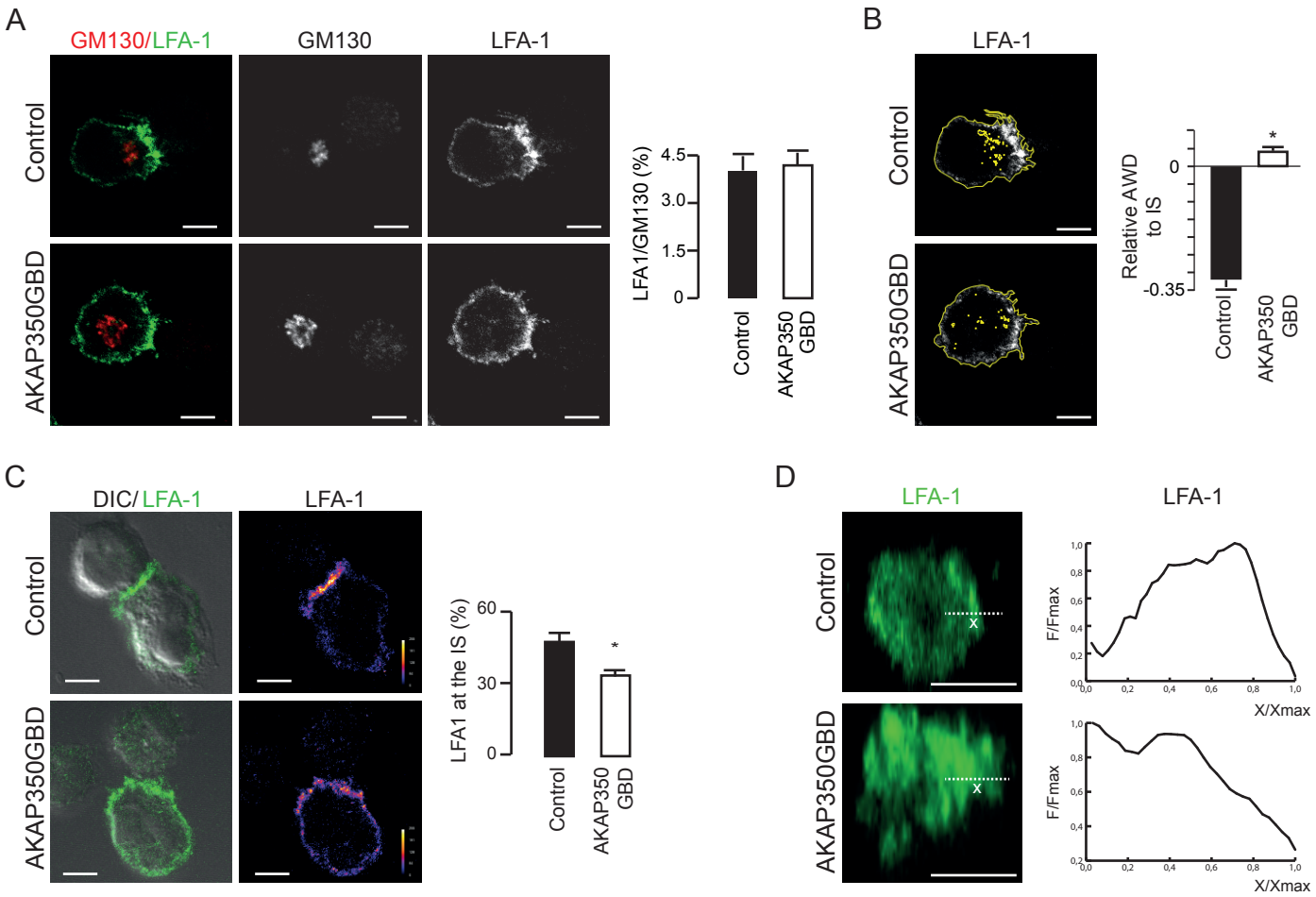

Figure 7. AKAP350 localization at the Golgi apparatus is required for IS maturation. Control and AKAP350GBD YTS cells were incubated with KT86 cells. A) Merge images show staining for LFA-1 (green, only positive for YTS cells) and GM130 (red). Bars represent the mean fraction of LFA-1 that colocalized with GM130 for 10 different cells. B) Images show LFA-1 staining (grey scale) and the ROIs delimiting the cells and the individual LFA-1 vesicles in yellow. Bars represent the mean difference between the average weigthed distance (AWD) from the intracellular LFA-1 vesicles to the IS and the distance from the cell centroid to the IS, relativized to the latter, representative of three independent experiments. At least 10 conjugates were analyzed for each experiment. Error bars represent SEM. C) Merge images show the DIC channel and LFA-1 staining (green) for YTS:KT86 conjugates. Individual LFA-1 channel is also shown in pseudocolor. Bars represent the mean fraction of LFA-1 fluorescence located at the IS, expressed as percentage of total cell fluorescence. More than 30 conjugates from 3 different experiments were analyzed. Error bars represent the SEM. D) Images show the XZ projection of the IS region corresponding to control and AKAP350GBD YTS cells. Dashed lines denote the radius of the IS where LFA-1 intensity of fluorescence was quantified. Charts represent the profile of intensity of fluorescence, representative of at least ten IS. Scale bars, 5 µm. *p<0.05.

et al., 2006; Stinchcombe et al., 2006), microtubule participation in the initial events that condition the maturation of NK lytic IS has not been thoroughly evaluated. In order to verify if AKAP350 dependent LFA-1 recruitment to the IS could be related to AKAP350 role in the modulation of microtubule dynamics, we analyzed if microtubule integrity was required for LFA-1 accumulation at the IS. We found that both cold-induced microtubule depolymerization in the presence of Nocodazole or suppression of microtubule dynamic instability with Taxol inhibited LFA-1 accumulation and distribution at the IS (Figure 8). It is noteworthy that, in the same conditions, the reorganization of the actin cytoskeleton at the IS was preserved.

Discussion

NK cell cytotoxicity requires extensive cytoskeleton remodeling and receptor reorganization at the IS. LFA-1 clustering at the IS is central, not only for the consolidation of NK adhesion to target cells, but also for the activation of signalling pathways that lead to lytic granule translocation towards the IS (Barber et al., 2004; Bryceson et al., 2005). Even though many studies have contributed to clarify the signalling pathways that promote LFA-1 conformational activation during NK interaction with sensitive target cells, the mechanisms leading to LFA-1 accumulation at the IS at these cells have not been elucidated so far. In the present study, we provide evidence that AKAP350 participates in NK cytolytic activity by facilitating LFA-1 recruitment to the lytic IS and, therefore, IS maturation. Regarding the mechanisms involved, our study revealed the presence of an intracellular pool of LFA-1 that polarizes to the IS in an AKAP350 manner, and provides evidence supporting a central role for the Golgi apparatus and its derived microtubules in LFA-1 polarization and organization at the IS.

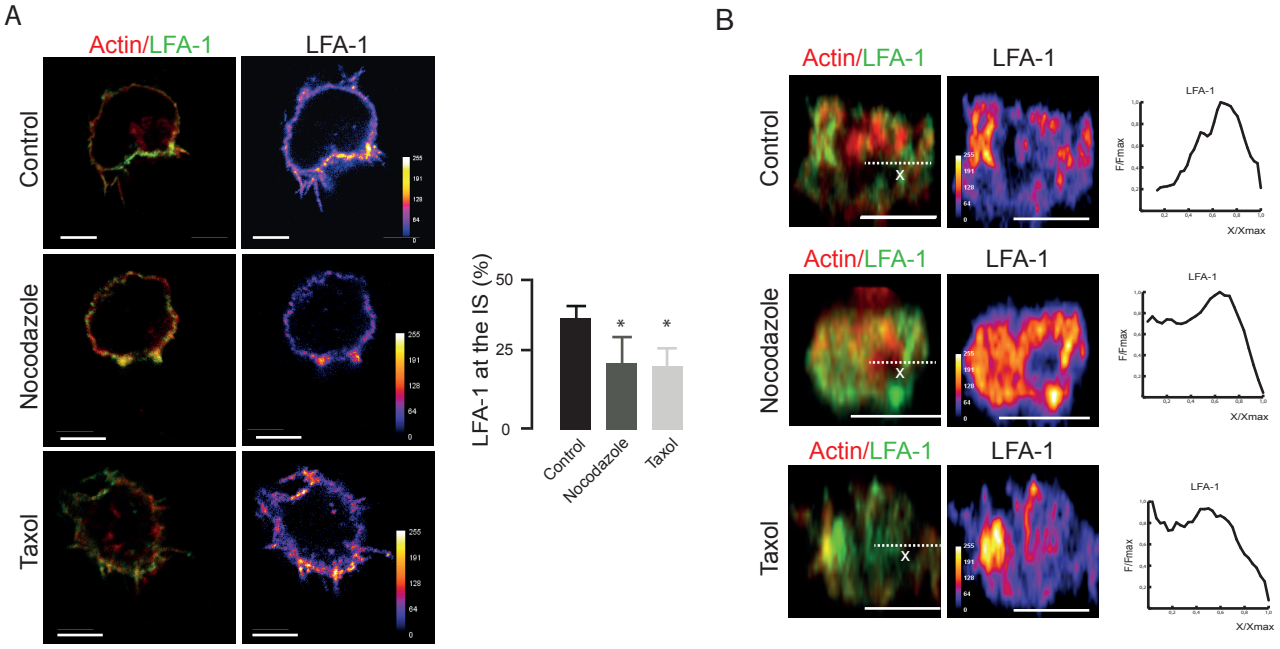

Figure 8. Microtubule dynamics is required for LFA-1 organization at the IS. Control YTS cells or YTS cells treated with nocodazole or taxol (see Materials and methods) were mixed with KT86 cells at a 2:1 ratio. A) Merge images show cell conjugates staining for actin (red) and LFA-1 (green). LFA-1 channel is also shown in pseudocolor. Bars represent the mean fraction of LFA-1 fluorescence located at the IS, expressed as percentage of total cell fluorescence. More than 30 conjugates from 3 different experiments were analyzed. Error bars represent the SEM. B) Merge images show x,z projections of the IS region corresponding to control and nocodazole or taxol treated YTS cells that were stained for actin (red) and LFA-1 (green). Dashed lines denote the radius of the IS where LFA-1 intensity of fluorescence was quantified. Charts represent the intensity profile of fluorescence quantified for the LFA-1 channel, representative of at least ten IS analyzed in three independent experiments. Scale bars, 5 μm. Error bars represent SEM. *$p<0.05$.

Our findings show that the decrease in AKAP350 expression leads to decreased NK cytolytic activity, which is associated with defective LFA-1 recruitment to the IS and concomitant inhibition of lytic granules translocation to the IS. Most of the information regarding LFA-1 redistribution at the cell surface originated in studies performed in T cells. The classical model proposes that conformational/ligand induced regulation of LFA-1 lateral motility can account for actin-dependent LFA-1 accumulation at the IS (Cairo et al., 2006). More recently, Kim and col. identified a novel intracellular LFA-1 pool, which actively redistributes to the surface of T cell:target cell interaction upon antigen stimulation (Capece et al., 2017). In the same line of evidence, previous studies performed in migrating T cells indicated that LFA-1-dependent migration decreases when intracellular vesicle transport is blocked, thus revealing the relevance of an intracellular pool of LFA-1 in the regulation of LFA-1 organization at the plasma membrane (Stanley et al., 2012). The characterization of that intracellular pool in T cells showed that it associates with early endosomes and with recycling endosomes (Ong et al., 2014; Samuelsson et al., 2017). Our results in NK cells indicate the presence of an intracellular pool of LFA-1, that was polarized towards the IS in control but not in AKAP350 KD cells. Interestingly, besides showing some identity with the recycling endosomes, that pool of LFA-1 positive vesicles show a prominent association with the Golgi apparatus, suggesting that this organelle could regulate LFA-1 trafficking to the IS in NK cells. Recent studies performed in T cells demonstrated that the Golgi apparatus regulates the two way vesicle trafficking to the IS of signaling proteins that are essential for IS maturation, thus revealing the participation of the Golgi apparatus in IS maturation in those cells (Carpier et al., 2018). Even though it is well established that the Golgi apparatus translocates to the IS during NK lytic response (Kupfer et al., 1983), to our knowledge, the role of this organelle in the development of NK lytic IS

has not been examined so far. Interestingly, our results showed that BFA treatment impairs LFA-1 accumulation at the IS, supporting our hypothesis that the Golgi apparatus regulates LFA-1 traffic to the IS and providing evidence, for the first time, for the participation of the Golgi apparatus in LFA-1 organization at the IS in NK cells.

Considering the results discussed above and the fact that, in NK cells conjugated to susceptible targets, AKAP350 is particularly enriched at the Golgi apparatus, we analyzed if there was a specific role of AKAP350 at this organelle. We found that AKAP350 delocalization from the Golgi apparatus inhibits LFA-1 accumulation and clustering at the IS, ratifying the role of the Golgi apparatus in IS maturation and underscoring the relevance of AKAP350 location at this organelle for the development of NK lytic IS. The presence of AKAP350 at the Golgi apparatus has been mainly associated with the role of this organelle in microtubule nucleation (Rivero et al, 2009, Ori-McKenney et al, 2012; Maia et al, 2013, Tonucci et al, 2018). In immune cells, microtubule nucleation has been typically attributed to the centrosome, which, in fact, is commonly denoted as the "microtubule organizing center" (MTOC). We found that NK cells nucleate microtubules both at the centrosome and at the Golgi apparatus and that the decrease in AKAP350 expression specifically inhibits microtubule nucleation at the Golgi. Those results are in agreement with previous studies that showed that the decrease in AKAP350 expression inhibits microtubule nucleation at the Golgi, without having an evident impact on centrosomal nucleation of microtubules (Larocca et al, 2006; Rivero et al, 2009; Tonucci et al, 2018). Golgi-derived microtubules are particularly stable, which correlates with their enrichment in post-translationally modified tubulin (reviewed in Sanders and Kaverina, 2015). In fact, the study that first characterized the Golgi apparatus as a MTOC showed that Golgi-nucleated microtubules become rapidly acetylated (Chabin-Brion et al., 2001). A recent study in

motile T cells showed that AKAP350 participates in microtubule nucleation at the centrosome and at extra-centrosomal nucleation centers (Ong et al., 2018). Although this study did not identify microtubule nucleation at the Golgi, it showed that the decrease in AKAP350 expression led to decreased levels of acetylated α-tubulin. In line with those studies, we found that either the decrease in AKAP350 expression or its delocalization from the Golgi apparatus elicited a decrease in acetylated α-tubulin levels, thus supporting AKAP350 participation in the organization of a pool of Golgi associated-highly acetylated microtubules. Different studies indicate that Golgi derived microtubules support the directionality of Golgi associated polarized trafficking (reviewed in Sanders and Kaverina, 2015). Our results showed that, similarly to the decrease in AKAP350 expression, AKAP350 delocalization from the Golgi inhibited LFA-1 vesicles polarization towards the IS. Considering the role of AKAP350 in microtubule nucleation at the Golgi, and the participation of this organelle in LFA-1 organization at NK-IS, those results sustain the participation of Golgi derived microtubules in LFA-1 directional traffic towards the IS. To further test this hypothesis, we assessed the role of the microtubule cytoskeleton in LFA-1 organization at the IS. We found that levels of nocodazole that actually inhibits NK cytotoxicity (Katz et al., 1982), induce a defect in LFA-1 organization at the IS. Orange et al have previously demonstrated that cell-surface receptor accumulation at the activating NK-IS was not disrupted with colchicine (Orange et al., 2003). Colchicine and nocodazole have similar mechanisms of action: both drugs bind to the β tubulin subunit blocking α/β heterodimers polymerization (Florian and Mitchison 2016). In our study, we additionally induced microtubule depolymerization by ice incubation, which leads to a more robust disruption of microtubule integrity and may explain the different outcomes between both experimental settings. Our results also showed that micromolar levels of

the microtubule stabilizing agent Taxol, which impedes microtubule growing and shortening events (Derry et al., 1995), also inhibited LFA-1 reorganization at the IS, providing further evidence that microtubule remodeling is essential for this process. It is noteworthy that, in our settings, neither Nocodazole nor Taxol treatment affect actin accumulation or organization, thus ruling out that the inhibition in LFA-1 organization at the IS could be secondary to microtubule effects on actin organization at this site.

Summarizing, the present study reveals a novel mechanism that conditions LFA-1 reorganization at the lytic IS with a direct impact on NK effector function, which involves AKAP350 and the Golgi apparatus. The relevance of a similar mechanism in the development of different types of IS or in immune cells migration constitutes an interesting matter for future studies.

Materials and methods

NK and target cell lines

The immortalized NK YTS cells [Drexler, and Matsuo. 2000] and KT86 cells, derived from the MHC class I-negative K562 erythroleukemia cell line stably expressing CD86 [Parry et al, 2003], used as susceptible target cells, were obtained from Dr. Jordan Orange lab (Texas Children's Hospital, Houston, TX, USA). Cells were maintained in RPMI medium 1640 supplemented with 10% FBS, 1% L-glutamine, 1% non-essentials amino acids and 1% streptomycin/ampicillin mixture at 37° C and 5% CO_2 atmosphere.

In order to prepare YTS cells with reduced expression of AKAP350 (AKAP350KD), we proceeded as we have described previously [Tonucci et al., 2015]. Constructs were made by annealing and ligating oligonucleotides targeting two specific AKAP350 sequences (shRNA1, 5′-CCCAGCTCACTGCTAATTT-3′; shRNA4,

5′-GCAAGAACTAGAACGAGAA-3′) or a scrambled control into the AgeI and EcoRI cloning sites of pLKO.1-puro vector (details at http://www.addgene.org). These constructs were sequenced and used to co-transfect human embryonic kidney 293 FT cells with Virapower lentiviral packaging mix (Invitrogen, Carlsbad, CA). The next day, transfection complexes were removed, and cells were allowed to produce virus for 24 h. Media containing viruses were collected and used to directly transduce YTS cells overnight. The cells were then allowed to recover for 24 h and subjected to puromycin selection (2 µg/ml) for 2 weeks. Silencing was confirmed by western blotting and immunofluorescence analyses.

In order to delocalize AKAP350 from the Golgi apparatus, the nucleotide sequence codifying for AKAP350(1-1229) (AKAP350GBD) was cloned into pInducer20 vector (details at http://www.addgene.org). The lentiviral particles were constructed as described above. Transduced YTS cells were subjected to G418 selection (1 µg/ml) for two weeks. AKAP350GBD expression was induced with Doxycycline (2 µg/ml) 24 h before the experiments.

CFSE-based Cytotoxic assay

In order to determine the lytic capacity of YTS cells, we proceed as described [Jedema et al. 2004]. KT86 cells were washed with PBS, resuspended at 2 x10^6 cells/mL and labeled with 300 nM CFSE (BD Horizont) for 15 min at 37°C. The reaction was stopped by the addition of an equal volume of fetal bovine serum (FCS), followed by a 2-min incubation at room temperature. CFSE-labeled target cells were washed twice and resuspended in RPMI complete medium. The cell concentration was adjusted to 5 x 10^5 cells/mL, and 100 µL/tube were plated in Eppendorf tubes. YTS cells were added at different effector:target ratios. Tubes were incubated in a humidified atmosphere of 5% CO2 and 37°C for 3 hours. For staining dead cells, propidium iodide (1 µg/mL) was

added, and samples were mixed properly and directly analyzed by flow cytometry using a BD FACSAria II flow cytometer. 10000 events were acquired for each sample. Double positive events for CFSE and PI were considered dead target cells. The percentage of specific lysis was calculated as follows: specific lysis (%) = [(Double positive cells - spontaneous dead cells) / CFSE positive cells] x 100.

FACS-based conjugation assay

YTS cells were washed with PBS, resuspended to 1 x 10^6 cells/ml and labeled with 1.5 mM Cell TrackerTM Deep Red (Invitrogen) for 20 min at 37° C. The reaction was stopped by the addition of an equal of fetal bovine serum, followed by a 5 min incubation at room temperature. After two washes with PBS, the YTS-labeled cells were resuspended in RPMI complete medium. Target cells were labeled with 300 nM CFSE (BD Horizon) as described above. Cells were combined at an effector to target ratio of 2:1 or 10:1 and incubated at 37º C for different periods. The samples were gently vortexed for 3 s and immediately fixed with 2% paraformaldehyde (PFA). Samples were run in triplicates and 50000 events were counted for each replicate. The frequency of double positive events was determined within the total cell population using FlowJo software. The following gating strategy was used: First, cells were gated to exclude debris. Compensation adjustments were made on the gated population using single-positive cells stained for either Cell TrackerTM Deep Red or CFSE. Gates were set to differentiate between the double positives, represented in G2, from the single positives and double negatives. The percentage of conjugated cells was calculated as follows: conjugated cells (%) = [Double positive cells / total cells] x 100.

Immunofluorescence

KT86 were labeled with 300 nM CFSE (BD Horizon) as described above. Conjugates between YTS cells and KT86 at a 2:1 ratio were established in suspension for 15 min at

37 ° C and adhered to poly-lysine-coated glass slides (Polyprep; Sigma-Aldrich) for additional 15 min. In experiments evaluating NK cell activation by means of specific activating receptors, poly-l-lysine coated glass slides were coated by overnight incubation with anti-CD28 (5 μg/mL, BDbioscience 554121) and/or ICAM-1 (5 μg/mL, Biolegend 552906) in PBS. Slides were washed, and NK cells were incubated on the slide for 30 min at 37 ° C. Non adherent cells were washed and cells adhering to the slide were fixed with 4% PFA at room temperature or methanol at -20° C. Fixed cells were blocked with 1% bovine serum albuminin/PBS, pH 7.4, for 10 min. When indicated, 0.3%Triton X-100 was added to the buffer to enhance cell permeabilization. Then, they were incubated for 2 h with mouse monoclonal antibody anti-LFA-1 (Biolegend 301202), anti-AKAP350 (Schmidt et al, 2001), anti-Perforin (Santa Cruz SC-136994) or anti-alpha tubulin (Sigma T5168) and rabbit monoclonal antibody anti γ-tubulin (Sigma-T5192), anti-GM130 (Abcam EP892Y) or anti-RAB11 (Abcam ab180504). The coverslips were washed, incubated for 1 h with the secondary antibodies conjugated to Alexa 488, Alexa 560 or Alexa 633 or with phalloidin-Alexa 568 (Molecular probes-A34055, 1:200) for actin staining and with 4′,6-diamidino-2-phenylindole (DAPI) and mounted with ProLong (Invitrogen). Fluorescence was detected using LSM880 confocal with an ObserverZ1 inverted microscope. Serial optical 0.4 μm thick sections were collected in the z-axis. Z-stacks were built, and projections were obtained using ImageJ tools. In preparing the figures, adjustment in brightness and contrast were equally applied to the entire images using Adobe Photoshop software to improve visualization of fluorescence.

Image analysis

Lytic granule convergence and centrosome and lytic granule polarization towards the IS. YTS:KT86 conjugates were permeabilized and stained with anti γ-tubulin, perforin

and DAPI, for lytic granules, centrosome and nucleus identification. The IS was defined as the cell to cell contact region identified in the images obtained by differential interference microscopy (DIC). The cell perimeter of the YTS cell forming the IS was drawn using the same images. At the *x,y* plane corresponding to the centrosome center, a threshold was set on the perforin or γ-tubulin channel to define the respective masks, which were used to automatically outline the centrosome or the lytic granule regions. The *x,y* coordinate values for the IS, the lytic granules, the centrosome, and the cell centroids were determined using the appropriate ImageJ tool and the distances from the lytic granules, the centrosome or the cell centroids to the IS centroid, or from the lytic granules to the centrosome centroid were calculated. In the case of lytic granules, an average area-weighted distance (AWD) was calculated for each cell by applying a modified use of Shepard's Method (Mentlik et al, 2010), using the formula:

$$AWD = \sum_{i=1}^{n} di \times \left[Ai \div \sum_{i=1}^{n} Ai \right]$$

where Ai is the area of each particular lytic granule region and di is the distance from this particle to the IS or the centrosome. This modification allowed weighting the distances by the area of each lytic granule region, which is important considering that, when they are close together, clusters of lytic granules could inappropriately be discerned as an individual granule of a larger area and, therefore, if a factor considering each granule area is not used, those granules could be under-represented. Alternatively, for analysis of lytic granules and centrosome translocation during specific LFA-1 mediated activation, the surface of YTS interaction with ICAM-1 coated slides was considered the IS site, and the distance was measured at the *y,z* plane. At least 30 cells from three independent experiments were analyzed for each condition.

LFA-1-vesicles polarization towards the IS. YTS:KT86 conjugates were permeabilized and stained with anti LFA-1, for LFA-1 vesicles identification. The IS and the cell regions were defined in the DIC images, as explained above. A threshold was set on the LFA-1 channel to define a mask, which was used to automatically outline regions corresponding to the LFA-1 vesicles. The IS, LFA-1 vesicles and the cell centroid were determined using the appropriate ImageJ tool and the distances from the LFA-1 vesicles or the cell centroids to the IS centroid were calculated. Similar to what we explained above for lytic granules, an average area-weighted distance (AWD) was calculated for each cell.

For LFA-1 accumulation at the IS, YTS cells conjugated with KT86 cells were analyzed. We used DIC images for IS and cell selections as we describe above. We measured average and total intensity of fluorescence at YTS IS and at the whole cell (T). The percentage of protein accumulation was calculated as the ratio IS*100/T.

For LFA-1 distribution within the IS, the image J tool reslice was used for x,z planes reconstruction of the IS region and the plugin Radial Profile (http://rsbweb.nih.gov/ij/plugins/radial-profile.html) was used for measuring the intensity of fluorescence at concentric circumferences beginning at the center towards the periphery of the IS.

Centrosomal localization of AKAP350 was determined in images obtained by confocal microscopy by setting a threshold on γ-tubulin channel to define a mask, which was used to automatically outline the centrosomal voxels, and a threshold on AKAP350 channel to define a mask to automatically outline total voxels for AKAP350 staining. Average and total intensity of fluorescence in the AKAP350 channels was measured in each region of interest, and the ratio of centrosomal and total cell levels calculated.

AKAP350 or LFA-1 association to the Golgi apparatus were determined in images obtained by confocal microscopy by setting a threshold on the GM130 channel to define a mask, which was used to automatically outline the Golgi pixels. Total intensity of fluorescence in the AKAP350 or LFA-1 channel was measured in each region of interest. In addition, total AKAP350 or LFA-1 levels were determined in the region corresponding to the YTS cell, and the percentage of AKAP350 or LFA-1 fluorescence at the Golgi apparatus calculated. A similar protocol was used to estimate LFA-1 association with the recycling endosomes, using Rab11 staining to define this compartment. AKAP350 colocalization with GM130 in AKAP350GBD cells was determined by estimating the Pearson´s coefficient using the Image J colocalization tools.

Immunoblotting

Cells were harvested at 400 *g* for 5 min at room temperature and washed with cold PBS. Pelleted cells were lysed in ice-cold lysis buffer (50 mM Tris-HCl [pH 7.5], 100 mM NaCl, 15 mM EDTA and 1% Triton X-100, with protease inhibitors) and subjected to two freeze–thaw cycles. Lysates were centrifuged at 1000 *g* for 5 min at 4° C, and the clear supernatants were conserved. Total protein concentrations were measured according to Lowry *et al*. (1951). Samples were heated for 10 min at 90 °C in sample buffer (20 mM Tris-HCl, pH 8.5, 1% SDS, 400 µM DTT, 10% glycerol). Samples containing equal amounts of proteins were subjected to SDS polyacrylamide gel electrophoresis (6–10% gradient to verify AKAP350 silencing or 10% otherwise). The proteins in the 6% gel were transferred to nitrocellulose membranes (Amersham Pharmacia Biotech), whereas the 10% gel proteins were transferred to polyvinyl difluoride membranes (Perkin Elmer Life Sciences). Blots were blocked with 5% non-fat dry milk in PBS, 0.3% Tween-20 (PBS-Tween). Nitrocellulose blots were then

probed with the monoclonal mouse anti-AKAP350 antibody (1:500), and polyvinyl difluoride membranes were probed with mouse monoclonal antibodies anti-α-tubulin (Sigma-T5168, 1:5000) or anti-CIP4 (BD Bioscience 612557). The blots were washed and incubated with the horseradish peroxidase-conjugated corresponding secondary antibodies, and bands were detected by enhanced chemiluminescence (Pierce, Thermo Scientific). Autoradiographs were obtained by exposing the blots to Kodak XAR film. The bands were quantitated by densitometry using the NIH Image J program.

YTS cells treatments

In order to assess the role of microtubules on the Immune Synapse formation, YTS cells were harvested and 2.10 ^{6} cells were treated for 1 hour with nocodazole (17 µM) on ice or for 1 hour with Taxol (10 µM) at room temperature and then allowed to form conjugates with KT86 cells at a 2:1 ratio for 15 min at 37° C. In order to evaluate the role of the Golgi apparatus in LFA-1 organization during IS formation, YTS cells were treated with Brefeldin A (5 µg/ml) for 30 min at 37 ° C. After Brefeldin A treatment, YTS cells were allowed to form conjugates with KT86 cells at a 2:1 ratio for 15 min at 37° C. In both cases, YTS cells without treatment were used as control for each experiment. Conjugates were analyzed by confocal microscopy as described above.

Ice recovery assay

A total of 2x10^{5} YTS cells were placed on poly-l-lysine-coated coverslips coated with IgG or with ICAM-1 and an anti-CD28 activating antibody and incubated for 30 minutes at 37°C. Then, coverslips were incubated on ice 50 min and allowed to recover at room temperature. For analysis of Golgi and centrosome nucleation of microtubules, cells were recovered for 3 or 7 minutes and immediately treated 45 s with extraction buffer (60 mM PIPES, 25 mM HEPES, 10 mM EGTA, 2 mM MgCl2, 0.1% Tritón X-100, pH 6.9, supplement with 0.25 nM nocodazole and 0.25 nM paclitaxel). Cells were

then fixed with methanol and stained with anti-GM130 and anti α-tubulin antibody (Sigma-T9026).

Acknowledgments

We thank Dr. Andrés Zucchetti for his critical discussion of the manuscript. This work was supported by Grants PUE 0089 from CONICET and PICT2015-2755 and PICT2016 from ANPCyT. The funders had no role in study design, data collection and analysis, decision to publish, or paper preparation.

Competing interests

There are not competing interests to declare.

References

Almada E, Tonucci FM, Hidalgo F, Ferretti A, Ibarra S, Pariani A, Vena R, Favre C, Girardini J, Kierbel A, Larocca MC. Akap350 Recruits Eb1 to The Spindle Poles, Ensuring Proper Spindle Orientation and Lumen Formation in 3d Epithelial Cell Cultures. Sci Rep. 2017; 7:14894. doi: https://doi.org/10.1038/s41598-017-14241-y

Barber DF, Faure M, Long EO. LFA-1 contributes an early signal for NK cell cytotoxicity. J Immunol. 2004; 173:3653-9. doi: https://doi.org/10.4049/jimmunol.173.6.3653.

Bryceson YT, March ME, Barber DF, Ljunggren HG, Long EO. Cytolytic granule polarization and degranulation controlled by different receptors in resting NK cells. J Exp Med. 2005; 202:1001-12. doi: https://doi.org/10.1084/jem.20051143.

Cairo CW, Mirchev R, Golan D. Cytoskeletal regulation couples LFA-1 conformational changes to receptor lateral mobility and clustering. Immunity 2006;25:297-308. doi: https://doi.org/10.1016/j.immuni.2006.06.012

Capece T, Walling BL, Lim K, Kim KD, Bae S, Chung HL, Topham DJ, Kim M. A novel intracellular pool of LFA-1 is critical for asymmetric CD8(+) T cell activation and differentiation. J Cell Biol. 2017; 216:3817-3829. doi: https://doi.org/10.1083/jcb.201609072

Carpier JM Carpier JM, Zucchetti AE, Bataille L, Dogniaux S, Shafaq-Zadah M, Bardin S, Lucchino M, Maurin M, Joannas LD, Magalhaes JG, Johannes L, Galli T, Goud B, Hivroz C. Rab6-dependent retrograde traffic of LAT controls immune synapse formation and T cell activation. J. Exp. Med. (2018) 215, 1245–1265. DOI: 10.1084/jem.20162042

Chabin-Brion K, Marceiller J, Perez F, Settegrana C, Drechou A, Durand G, Poüs C . The Golgi complex is a microtubule-organizing organelle. Mol Biol Cell. 2001; 12:2047-60. DOI: 10.1091/mbc.12.7.2047

Chardin P, McCormick F. Brefeldin A: The Advantage of Being Uncompetitive. Cell. 1999; 97:153-155. DOI: 10.1016/s0092-8674(00)80724-2

Chen X, Allan DS, Krzewski K, Ge B, Kopcow H, Strominger JL. CD28-stimulated ERK2 phosphorylation is required for polarization of the microtubule organizing center and granules in YTS NK cells. Proc. Natl. Acad. Sci. USA. 2006; 103:10346–10351. DOI: 10.1073/pnas.0604236103

Derry WB, Wilson L, Jordan MA. Substoichiometric Binding of Taxol Suppresses Microtubule Dynamics. Biochemistry 1995,34, 2203-2211. DOI: 10.1021/bi00007a014

Drexler, H. G., Y. Matsuo. 2000. Malignant hematopoietic cell lines: in vitro models for the study of natural killer cell leukemia-lymphoma. Leukemia 14: 777-782. DOI: 10.1038/sj.leu.2401778

El Din El Homasany BS, Volkov Y, Takahashi M, Ono Y, Keryer G, Delouvée A, Looby E, Long A, Kelleher D. 2005. The scaffolding protein CG-NAP/AKAP450 is a critical integrating component of the LFA-1-induced signaling complex in migratory T cells. J Immunol. 175:7811-8. DOI: 10.4049/jimmunol.175.12.7811

Florian S, Mitchison TJ. Anti-Microtubule Drugs. Methods Mol Biol. 2016; 1413:403-21. doi: 10.1007/978-1-4939-3542-0_25. DOI: 10.1007/978-1-4939-3542-0_25

Fong A, Durkin A, and Lee H. Int. The Potential of Combining Tubulin-Targeting Anticancer Therapeutics and Immune Therapy. J. Mol. Sci. 2019, 20, 586; doi:10.3390/ijms20030586. DOI: 10.3390/ijms20030586

Grimaldi AD, Fomicheva M, Kaverina I. Ice recovery assay for detection of Golgi-derived microtubules. Methods Cell Biol. 2013; 118:401-15. DOI: 10.1016/B978-0-12-417164-0.00024-0

Hoffmann SC, Cohnen A, Ludwig T, Watzl C. 2B4 engagement mediates rapid LFA-1 and actin-dependent NK cell adhesion to tumor cells as measured by single cell force spectroscopy. J Immunol. 2011; 186:2757-64. doi: https://doi.org/10.4049/jimmunol.1002867.

Hurtado L, Caballero C, Gavilan MP, Cardenas J, Bornens M, Rios RM. Disconnecting the Golgi ribbon from the centrosome prevents directional cell migration and ciliogenesis. J Cell Biol. 2011 May 30;193(5):917-33. DOI: 10.1083/jcb.201011014

Jedema I, van der Werff NM, Barge RM, Willemze R, Falkenburg JH.. New CFSE-based assay to determine susceptibility to lysis by cytotoxic T cells of leukemic

precursor cells within a heterogeneous target cell population. *Blood* 103.7 (2004): 2677-2682. DOI: 10.1182/blood-2003-06-2070

Katz P, Zaytoun AM and Lee J H Jr. Mechanisms of human cell-mediated cytotoxicity. III. Dependence of natural killing on microtubule and microfilament integrity. J Immunol 1982, 129: 2816-2825.

Kupfer A, Dennert G, Singer SJ. Polarization of the Golgi apparatus and the microtubule-organizing center within cloned natural killer cells bound to their targets. Proc Natl Acad Sci USA 1983; 80: 7224–7228. DOI: 10.1073/pnas.80.23.7224

Kolobova E, Roland JT, Lapierre LA, Williams JA, Mason TA, Goldenring JR. The C-terminal region of A-kinase anchor protein 350 (AKAP350A) enables formation of microtubule-nucleation centers and interacts with pericentriolar proteins. J Biol Chem. 2017; 292: 20394–20409. DOI: 10.1074/jbc.M117.806018

Lagrue K, Carisey A, Oszmiana A, Kennedy PR, Williamson DJ, Cartwright A, Barthen C, Davis DM.. The central role of the cytoskeleton in mechanisms and functions of the NK cell immune synapse. Immunological Reviews 2013. Vol. 256: 203–221. DOI: 10.1111/imr.12107

Larocca MC, Jin M, Goldenring JR. AKAP350 modulates microtubule dynamics. Eur J Cell Biol. 2006; 85:611-9. DOI: 10.1016/j.ejcb.2005.10.008

Maia AR, Zhu X., Miller P., Gu G., Maiato H., Kaverina I. (2013). Modulation of Golgi-associated microtubule nucleation throughout the cell cycle. Cytoskeleton 70, 32–43. 10.1002/cm.21079. DOI: 10.1002/cm.21079

Mace EM, Dongre P, Hsu H-T, Sinha P, James AM, Mann SS, Forbes LR, Watkin LB, Orange JS. Cell biological steps and checkpoints in accessing NK cell cytotoxicity. Immunol Cell Biol. 2014; 92: 245–255. DOI: 10.1038/icb.2013.96

Mentlik AN, Sanborn KB, Holzbaur EL, Orange JS. Rapid lytic granule convergence to the MTOC in natural killer cells is dependent on dynein but not cytolytic commitment. Mol Biol Cell. 2010; 21:2241-56. DOI: https://doi.org/10.1091/mbc.e09-11-0930

Ong ST, Chalasani MLS, Fazil MHUT, Prasannan P, Kizhakeyil A, Wright GD, Kelleher D, Verma NK. Centrosome- and Golgi-Localized Protein Kinase N-Associated Protein Serves As a Docking Platform for Protein Kinase A Signaling and Microtubule Nucleation in Migrating T-Cells. Front Immunol. 2018; 9:397. DOI: https://doi.org/10.3389/fimmu.2018.00397

Ong ST, Freeley M, Skubis-Zegadlo J, Fazil MH, Kelleher D, Fresser F, Baier G, Verma NK, Long A, Phosphorylation of Rab5a protein by protein kinase CD is crucial for T-cell migration. J. Biol. Chem. 289, 19420–19434 (2014). doi: 10.1074/jbc.M113.545863

Orange JS. Formation and function of the lytic NK-cell immunological synapse. Nat Rev Immunol. 2008 Sep;8(9):713-25. doi: https://doi.org/10.1038/nri2381

Orange JS, Harris KE, Andzelm MM, Valter MM, Geha RS, Strominger JL. The mature activating natural killer cell immunologic synapse is formed in distinct stages. Proc Natl Acad Sci U S A. 2003; 100:14151-6. doi: https://doi.org/10.1073/pnas.1835830100

Ori-McKenney, K. M., Jan, L. Y., & Jan, Y.-N. (2012). Golgi outposts shape dendrite morphology by functioning as sites of acentrosomal microtubule nucleation in neurons. Neuron, 76, 921– 930. DOI: 10.1016/j.neuron.2012.10.008

Parry, Richard V., et al. CD28 and inducible costimulatory protein Src homology 2 binding domains show distinct regulation of phosphatidylinositol 3-kinase, Bcl-xL, and IL-2 expression in primary human CD4 T lymphocytes. The Journal of immunology, 2003, vol. 171, no 1, p. 166-174. DOI: 10.4049/jimmunol.171.1.166

Rivero S, Cardenas J, Bornens M, Rios RM. Microtubule nucleation at the cis-side of the Golgi apparatus requires AKAP450 and GM130. EMBO J. 2009, 281016-28. DOI: 10.1038/emboj.2009.47

Robles-Valero J, Martín-Cófreces NB, Lamana A, Macdonald S, Volkov Y, Sánchez-Madrid F. (2010) Integrin and CD3/TCR activation are regulated by the scaffold protein AKAP450. Blood. 115:4174-84. DOI: 10.1182/blood-2009-12-256222

Samuelsson M, Potrzebowska K, Lehtonen J, Beech JP, Skorova K, Uronen-Hansson H, Svensson L,. RhoB controls the Rab11-mediated recycling and surface reappearance of LFA-1 in migrating T lymphocytes. Sci Signal 2017; 10:eaai8629. doi: https://doi.org/10.1126/scisignal.aai8629

Sanders AA, Kaverina I. Nucleation and dynamics of Golgi-derived microtubules. Front Neurosci. 2015;9:431. doi: 10.3389/fnins.2015.00431. DOI: 10.3389/fnins.2015.00431

Schmidt PH, Dransfield DT, Claudio JO, Hawley RG, Trotter KW, Milgram SL,et al. AKAP350, a multiply spliced protein kinase A-anchoring protein associated with centrosomes. J Biol Chem. 1999; 274:3055-66. DOI: 10.1074/jbc.274.5.3055

Stanley P, Tooze S, Hogg N, A role for Rap2 in recycling the extended conformation of LFA-1 during T cell migration. Biol. Open 1, 1161–1168 (2012). DOI: https://doi.org/10.1242/bio.20122824

Stinchcombe JC, Majorovits E, Bossi G, Fuller S, Griffiths GM. Centrosome polarization delivers secretory granules to the immunological synapse. Nature. 2006; 443:462-5. doi: https://doi.org/10.1038/nature05071.

Takahashi M, Yamagiwa A, Nishimura T, Mukai H, Ono Y. Centrosomal Proteins CG-NAP and Kendrin Provide Microtubule Nucleation Sites by Anchoring γ-Tubulin Ring

Complex. Mol Biol Cell. 2002; 13: 3235–3245. DOI: https://doi.org/10.1091/mbc.e02-02-0112

Tonucci FM, Ferretti A, Almada E, Cribb P, Vena R, Hidalgo F, Favre C, Tyska MJ, Kaverina I, Larocca MC. Microtubules regulate brush border formation. J Cell Physiol. 2018; 233:1468-1480. DOI: 10.1002/jcp.26033. DOI: https://doi.org/10.1002/jcp.26033

Tonucci FM, Hidalgo F, Ferretti A, Almada E, Favre C, Goldenring JR, Kaverina I, Kierbel A, Larocca MC. Centrosomal AKAP350 and CIP4 act in concert to define the polarized localization of the centrosome and Golgi in migratory cells. J Cell Sci. 2015; 128:3277-89. DOI: https://doi.org/10.1242/jcs.170878.

Urlaub D, Höfer K, Müller ML, Watzl C. LFA-1 Activation in NK Cells and Their Subsets: Influence of Receptors, Maturation, and Cytokine Stimulation. J Immunol. 2017; 198:1944-1951. doi: https://doi.org/10.4049/jimmunol.1601004.

Vyas YM, Mehta KM, Morgan M, Maniar H, Butros L, Jung S, Burkhardt JK, Dupont B. Spatial organization of signal transduction molecules in the NK cell immune synapses during MHC class I-regulated non-cytolytic and cytolytic interactions. J Immunol. 2001; 167:4358-67. DOI: https://doi.org/10.4049/jimmunol.167.8.4358.

FIGURE LEGENDS

Figure 1. AKAP350 localization in YTS cells. Isolated YTS cells or YTS:KT86 conjugates were stained and analyzed by confocal microscopy as described in Materials and Methods. A,B) Merge images show YTS cells (upper row) or YTS:KT86 conjugates (lower row) staining for AKAP350 (red) and γ-tubulin (A) or GM130 (B) (green). Asterisk denotes YTS cells in YTS:KT86 conjugates. Bars represent the mean fraction of AKAP350 fluorescence present at centrosomes (A) or at the Golgi apparatus (B) in isolated or conjugated YTS cells, expressed as a percentage of total AKAP350-

fluorescence. Results are representative of three independent experiments. At least 20 cells were analyzed for each experiment. Error bars represent SEM. *p < 0.05. Scale bars, 5 μm.

Figure 2. Reduction of AKAP350 expression levels diminishes YTS cells' cytotoxicity. Two different specific shRNAs (shRNA1 and shRNA4) were used to generate YTS cells with decreased AKAP350 expression (AKAP350KD1 and AKAP350KD2, respectively), as described in Materials and methods. A) Western blot analysis of AKAP350 expression in control, AKAP350KD1 and AKAP350KD2 YTS cells. CDC42-interacting protein 4 (CIP4) was used as loading control. B,C) KT86 cells were stained with CFSE and mixed with YTS cells at effector: target ratios of 2:1 (B) or 10:1 (C). After the incubation period, cells were stained with PI and analyzed by flow cytometry. YTS cytotoxic activity was estimated as the fraction of total CFSE positive events that were also positive for PI. Bars chart represents the mean percentage of double positive events for control, AKAP350KD1 and AKAP350KD2 cells, representative of three independent experiments. Error bars represent SEM. *p < 0.05.

Figure 3. AKAP350 is required for lytic granule convergence and centrosome and GA polarization during YTS cells activation. Control and AKAP350KD YTS cells were incubated with CFSE labeled KT86 cells at a 2:1 ratio. Cell conjugates were fixed, stained and analyzed by confocal microscopy. A) Merge images show staining for DAPI (blue) and perforin (cyan) and γ-tubulin (red) . The second and third columns show the localization of the centrosome, as delimited with an automatic selection tool, and the localization of the lytic granules centroids (second column) or the lytic granules area (third column), visualized using a specific Image J tool, corresponding with the boxed cell from the first column. The bars represents the mean area weighted distance (AWD) from the lytic granules to the IS or to the centrosome, calculated as described in

Materials and methods. B) Merge images show staining for DAPI (blue), AKAP350 (red) and γ-tubulin (cyan) . White arrows indicate the position of γ-tubulin-labeled centrosomes in YTS cells. Bars represent the mean distance from the centrosome to the IS. Results are representative of four (A) or five (B) independent experiments. At least 30 conjugates were analyzed for each experiment. Error bars represent SEM. Scale bars, 5 μm. *$p<0.05$.

Figure 4. Reduction of AKAP350 expression levels results in defective LFA-1 organization at the IS. A) Control and AKAP350KD YTS cells were incubated with CFSE labeled KT86 cells at a 2:1 ratio. Merge images show YTS:KT86 conjugates staining for LFA-1 (red, only positive for YTS cells) and DAPI (blue). LFA-1 channel is also shown in pseudocolor. Bars represent the mean area positive for LFA-1 at the IS and the average intensity of LFA-1 fluorescence at the IS relative to the average intensity of LFA-1 fluorescence at the cell for four independent experiments. At least 30 conjugates were analyzed for each experiment. Error bars represent SEM. B) Control and AKAP350KD YTS cells were activated using coverslips coated with ICAM-1. Merge images show LFA-1 (green) and DAPI (blue) staining. LFA-1 channel is also shown in pseudocolor. White dashed lines indicate the cell surface in contact with the coverslip. Bars represent the mean fraction of LFA-1 fluorescence located at the cell surface in contact with the ICAM-1 coated coverslip, expressed as the percentage of total cell fluorescence representative of three independent experiments. At least 30 conjugates were analyzed for each experiment. Error bars represent SEM. C) Images show the X-Z projection of the IS region corresponding to control and AKAP350KD YTS cells. LFA-1 staining is shown in green and in pseudocolor. Dashed lines denote the radius of the IS where LFA-1 intensity of fluorescence was quantified. Charts represent the intensity profile of fluorescence, representative of at least ten IS analyzed

in three independent experiments. D) Control and AKAP350KD YTS cells were activated using coverslips coated with ICAM-1. Merge images show g-tubulin (green), perforin (red) and DAPI (blue) staining. The second column shows the binarized image of the perforin channel, with the ROI corresponding to the centrosome indicated in green. Bars represent the mean average weighted distance (AWD) between the lytic granules and the centrosome (first chart) or between the centrosome and the ICAM-1 coated surface (second chart), representative of three independent experiments. Scale bars, 5 μm (A,B,D) or 2.5 μm (C). *$p<0.05$.

Figure 5. LFA-1 is expressed intracellularly and its redistribution to the IS is dependent on the integrity of the Golgi apparatus. A-C) Control (A-C) and AKAP350KD (A) YTS cells were incubated with KT86 cells at a 2:1 ratio. Cell conjugates were fixed, stained and analyzed by confocal microscopy. A) Images show LFA-1 staining (grey scale) and the ROIs delimiting YTS cells and the individual LFA-1 vesicles in yellow. Bars represent the mean difference between the average weighted distance (AWD) from the intracellular LFA-1 vesicles to the IS and the distance from the cell centroid to the IS, relativized to the latter, representative of three independent experiments. At least 10 conjugates were analyzed for each experiment. Error bars represent SEM. B,C) Merge images show staining for LFA-1 (green) and Rab11 (red, B) or GM130 (red, C) and the x,z orthogonal view of the boxed areas at the ordinate indicated with dashed lines. D-E) YTS cells were treated with brefeldin A (BFA) as described in Material and methods. Control or BFA treated YTS cells were incubated with KT86 cells. D) Merge images show staining for LFA-1 (green) and GM130 (gray). LFA-1 channel is also shown in pseudocolor. Bars represent the mean fraction of LFA-1 fluorescence located at the IS, expressed as percentage of total cell fluorescence for the LFA-1 channel, representative of three independent experiments. At least 8 conjugates were analyzed for each

experiment. Error bars represent SEM. E) Images show the x,z projection of the IS region corresponding to control and BFA treated YTS cells. Dashed lines denote the radius of the IS where LFA-1 intensity of fluorescence was quantified. Charts represent the intensity profile of fluorescence, representative of at least ten IS. Asterisks indicate YTS cells (D-E). Scale bars, 5 μm. *p<0.05.

Figure 6. AKAP350 is essential for microtubules nucleation at the Golgi apparatus in activated YTS cells. A) Control and AKAP350KD YTS cells were activated for 30 minutes using coverslips coated with ICAM-1 and anti-CD28 antibody. Merge images show staining for GM130 (red) and α-tubulin (green). Bar charts represent the mean fraction of α-tubulin fluorescence that colocalized with GM130, expressed as percentage of total cell fluorescence. B) Control YTS cells were seeded on coverslips coated ICAM-1 and the activating anti-CD28 antibody (activating conditions) or with IgG (resting conditions) for 30 minutes and then subjected to ice recovery assay. C) Control or AKAP350KD YTS cells were activated on coverslips coated with ICAM-1 and the activating anti-CD28 antibody for 30 minutes and then subjected to ice recovery assays. B, C) Merge images show staining for GM130 (red) and α-tubulin (green), and the orthogonal views of the x,z reslice at the ordinate level indicated with dashed lines, for cells fixed at 3 min (B) or 7 min (C) of recovery. The insets show a higher amplification of the boxed areas, for better visualization of microtubule association to the Golgi apparatus. Bar charts represent the mean fraction of α-tubulin fluorescence associated to each organelle, expressed as percentage of total cell fluorescence for the α-tubulin channel (B,C) and the mean number of microtubules derived from the centrosome or from the Golgi apparatus (C), representative of three independent experiments. At least 10 cells were analyzed for each experiment. Error bars represent SEM. Scale bars, 5 μm. *p<0.05.

Figure 7. AKAP350 localization at the Golgi apparatus is required for IS maturation. Control and AKAP350GBD YTS cells were incubated with KT86 cells. A) Merge images show staining for LFA-1 (green, only positive for YTS cells) and GM130 (red). Bars represent the mean fraction of LFA-1 that colocalized with GM130 for 10 different cells. B) Images show LFA-1 staining (grey scale) and the ROIs delimiting the cells and the individual LFA-1 vesicles in yellow. Bars represent the mean difference between the average weighted distance (AWD) from the intracellular LFA-1 vesicles to the IS and the distance from the cell centroid to the IS, relativized to the latter, representative of three independent experiments. At least 10 conjugates were analyzed for each experiment. Error bars represent SEM. C) Merge images show the DIC channel and LFA-1 staining (green) for YTS:KT86 conjugates. Individual LFA-1 channels are also shown in pseudocolor. Bars represent the mean fraction of LFA-1 fluorescence located at the IS, expressed as percentage of total cell fluorescence. More than 30 conjugates from 3 different experiments were analyzed. Error bars represent the SEM. D) Images show the XZ projection of the IS region corresponding to control and AKAP350GBD YTS cells. Dashed lines denote the radius of the IS where LFA-1 intensity of fluorescence was quantified. Charts represent the intensity profile of fluorescence, representative of at least ten IS. Scale bars, 5 μm. *$p<0.05$.

Figure 8. Microtubule dynamics is required for LFA-1 organization at the IS. Control YTS cells or YTS cells treated with nocodazole or taxol (see Materials and methods) were mixed with KT86 cells at a 2:1 ratio. A) Merge images show cell conjugates staining for actin (red) and LFA-1 (green). LFA-1 channel is also shown in pseudocolor. Bars represent the mean fraction of LFA-1 fluorescence located at the IS, expressed as percentage of total cell fluorescence. More than 30 conjugates from 3 different experiments were analyzed. Error bars represent the SEM. B) Merge images show *x,z*

projections of the IS region corresponding to control and nocodazole or taxol treated YTS cells that were stained for actin (red) and LFA-1 (green). Dashed lines denote the radius of the IS where LFA-1 intensity of fluorescence was quantified. Charts represent the intensity profile of fluorescence quantified for the LFA-1 channel, representative of at least ten IS analyzed in three independent experiments. Scale bars, 5 μm. Error bars represent SEM. *$p<0.05$.